Revista GEOCIÊNCIAS

unesp

ISSN: 1980-900X (online)

MODELING AND INSTRUMENTATION DATA ANALYSIS FROM EXCAVATION SLOPE OF THE MISICUNI DAM SPILLWAY (BOLIVIA): A CASE STUDY

ANÁLISE DE DADOS DE MODELAGEM E INSTRUMENTAÇÃO DO TALUDE DE ESCAVAÇÃO DO VERTEDOURO DA BARRAGEM DE MISICUNI (BOLÍVIA): UM ESTUDO DE CASO

Murilo da Silva ESPÍNDOLA[1], André Bianchi MATTOS[2], Roberto Borges MORAES[2], João Raphael LEAL[2], Vinícius Roberto de AGUIAR[3], Ariel Henrique POZZOBON[4]

[1]Universidade Federal de Santa Catarina. Programa de Pós-Graduação em Geologia. Núcleo de Pesquisas Geológicas – Florianópolis – SC. E-mail: murilo.espindola@ufsc.br
[2]Nova Engevix Engenharia e Projetos S/A. Rodovia Admar Gonzaga, 440 - Itacorubi, Florianópolis – SC. E-mails: mattos646@gmail.com; roberto.moraes@novaengevix.com.br; joao.leal@novaengevix.com.br
[3]Estelar Engenheiros Associados Ltda. Rod. José Carlos Daux, 500. João Paulo. Florianópolis – SC. E-mail: viniciusrag@yahoo.com.br
[4]DAM Projetos de Engenharia. Rua Marechal Hermes, 520. Gutierrez., Belo Horizonte – MG. E-mail: arielhpozzobon@gmail.com

RESUMO - A análise de estabilidade de taludes é de fundamental importância em projetos de infraestrutura, não importa seu tamanho. A falha de um talude tem um grande impacto econômico e ambiental e pode inviabilizar o projeto, causando danos irreparáveis ao meio ambiente e à vida. Portanto, a análise de estabilidade de taludes tem como objetivo avaliar a possibilidade de um talude sofrer movimentos de massa e propor soluções de estabilização. Esta pesquisa focou na obtenção dos parâmetros de resistência dos materiais encontrados no talude de escavação do vertedouro da Barragem de Misicuni aplicando o método de análise reversa e usando dados de instrumentação deformacional. A modelagem de parâmetros pode dar suporte a projetos futuros em termos de comportamento mecânico e segurança para a Barragem de Misicuni, além de projetos de engenharia subsequentes em massas de rochas sedimentares deformadas por influência tectônica. A Barragem Misicuni faz parte do Projeto Múltiplo Misicuni localizado no departamento de Cochabamba, parte central da Bolívia. Este projeto consiste em usar água das bacias dos rios Misicuni, Viscachas e Putucuni. Para realizar este artigo, três investigações de núcleo de perfuração foram usadas ao longo da seção de análise, bem como dados de leitura de dois inclinômetros instalados na escavação do talude de bancada, levantamento topográfico e 39 testes de compressão uniaxial em amostras coletadas dos núcleos de perfuração. Inclinômetros são instrumentos comumente utilizados para monitorar taludes de solo ou rocha, e auxiliam na determinação da superfície de falha e estimativa da velocidade de movimentação. O uso de dados de inclinômetros e modelagem geológica possibilitou analisar e obter parâmetros de tensão e deformação ocorridos durante as fases de escavação, por meio da aplicação da análise do Método dos Elementos Finitos (MEF), que permitiu comparar os resultados previstos e observados durante a execução e conclusão do local. Portanto, este artigo apresenta os parâmetros de resistência obtidos por meio de retroanálise usando dados de deformação obtidos de instrumentação de campo em um contexto de geologia estrutural complexa.
Palavras-chave: Maciço rochoso. Estabilidade de taludes. Instrumentação. MEF.

ABSTRACT - Slope stability analysis is of fundamental importance in infrastructure projects no matter its size. The failure of a slope has a major economic and environmental impact and can turn the project unfeasible, causing irreparable damage to the environment and life. Therefore, slope stability analysis aims to evaluate the possibility of a slope suffering mass movements and to propose stabilization solutions. This research focused on obtaining the resistance parameters of the materials found in the excavation slope of the Misicuni Dam spillway applying the back analysis method and using deformational instrumentation data. The parameter modeling can support future projects in terms of mechanical behavior and safety for the Misicuni Dam in addition to subsequent engineering projects in sedimentary rock masses deformed by tectonic influence. The Misicuni Dam is part of the Misicuni Multiple Project located in the Cochabamba department, central part of Bolivia. This project consists of using water from the Misicuni, Viscachas and Putucuni river basins. To carry out this paper, three drill core investigation were used along the analysis section, as well as read out data from two inclinometers installed on the bench slope excavation, topographic survey and 39 uniaxial compression tests on samples collected from the drill cores. Inclinometers are instruments commonly used to monitor soil or rock slopes, and help to determine the failure surface and estimate the speed of movement. The use of inclinometer data and geological modeling made it possible to analyze and obtain stress and strain parameters that occurred during the excavation phases, by applying Finite Element Method (FEM) analysis, which allowed to compare the predicted and observed results during the execution and completion of the site. Therefore, this paper presents the resistance parameters obtained through back analysis using deformation data obtained from field instrumentation in a context of complex structural geology.
Keywords: Rock Mass. Slope Stability. Instrumentation. FEM.

INTRODUCTION

Dams are structures that have contributed to the progress of humanity since ancient times. They were the first man-made structures to create water reservoirs for human supply. Over time, the use of reservoirs has diversified, with wide-ranging uses such as hydropower generation, navigation, recreation, flood control and irrigation.

However, over time several accidents have occurred involving this type of work, with around 60% of dam accidents being related to geotechnical problems, including foundation problems, settlements, high pore pressures, poor quality materials and slope slides (Jansen, 1983; Pereira, 2020).

The Misicuni Multiple Project is in the province of Cochabamba (Bolivia) and consists of harnessing the waters of the Misicuni, Viscachas and Putucuni river basins, on the other side of the Tunari mountain range, by creating a reservoir.

The main goal is to supply potable water to the urban populations of Cochabamba's Central Valley, use it in agriculture and hydropower generate. It is a project that aims to improve the availability of water in the Cochabamba Central Valley, bringing economic, social and cultural development to the region. The dam for impounding the water comprises an arrangement made up of rockfill with a concrete face for sealing, and a spillway which is located on the left bank.

The excavation of the channel and slopes for the spillway was carried out in sedimentary rocks with complex structural geology. A global collapse of these slopes, especially after completion of the site, could mobilize a large amount of material towards the rockfill, thus compromising the safety of the dam.

Therefore, understanding the mechanical behavior of the Misicuni Dam spillway excavation slope is essential in terms of safety and good stability performance. In this respect, deformation and resistance parameters can contribute to more reliable mathematical modeling of safety factors, including those based on the Limit-Equilibrium Theory.

The evaluation of instrumentation data, stresses and displacements, as well as previously determined variables, allows modeling and application of back analysis methods, which can provide support for future projections in terms of mechanical behavior and safety for this dam

GEOLOGICAL SETTINGS AND PROJECT BACKGROUND

Geological context

The Misicuni Dam is located in the Cordillera Oriental (Eastern Mountain Range), near the Cochabamba Valley, which has a municipality of the same name. The Cochabamba Valley is divided into three morphologically distinct zones: the flat zone, the hillside zone and the mountainous zone, where the Misicuni dam is located. The mountainous zone includes the Tunari and Mazo Cruz mountain ranges to the north and west of the valley and hills on the south and southeast sides.

The tectonic evolution of the Andean region is extremely complex, including throughout its history land accretions, rifting, orogenic episodes and the development of a highly shortened back-arc belt (Rojas Vera et al., 2019).

Study area and geological setting

The location of the Misicuni Multiple Project in the province of Cochabamba, central Bolivia, is shown in figure 1-B. The main objectives of the project are to supply potable water to the urban populations of the Cochabamba Central Valley, irrigation water for agriculture in the agricultural catchment area and electricity production of 80 MW to 120 MW for the National Interconnected System.

The Misicuni Dam is a concrete-faced rockfill dam with a height of 120 m and a crest length of 490 m at an elevation of 3782 m above sea level (Figure 2). The upstream slope has a gradient of 1.5H:1.0V and the downstream slope 1.5H:1.0V with a 6.0 m wide berm that develops from the 3675 m elevation.

The Misicuni dam is located in the Tunari mountain range and its structural configuration includes the Misicuni anticline to the east and the Uyuni syncline on its western flank (Figure 1-C).

The continuity between the anticline and the syncline is interrupted by the Misicuni reverse fault. The landscape of the dam site is the result of the tectonic action of major faults, mainly the Misicuni reverse fault, which, when combined with the erosive action of the river, cuts through the geological structures forming valleys with steep slopes on both sides (Leal et al., 2012).

There are Ordovician and Silurian rocks in the region, as well as Quaternary deposits. The upper

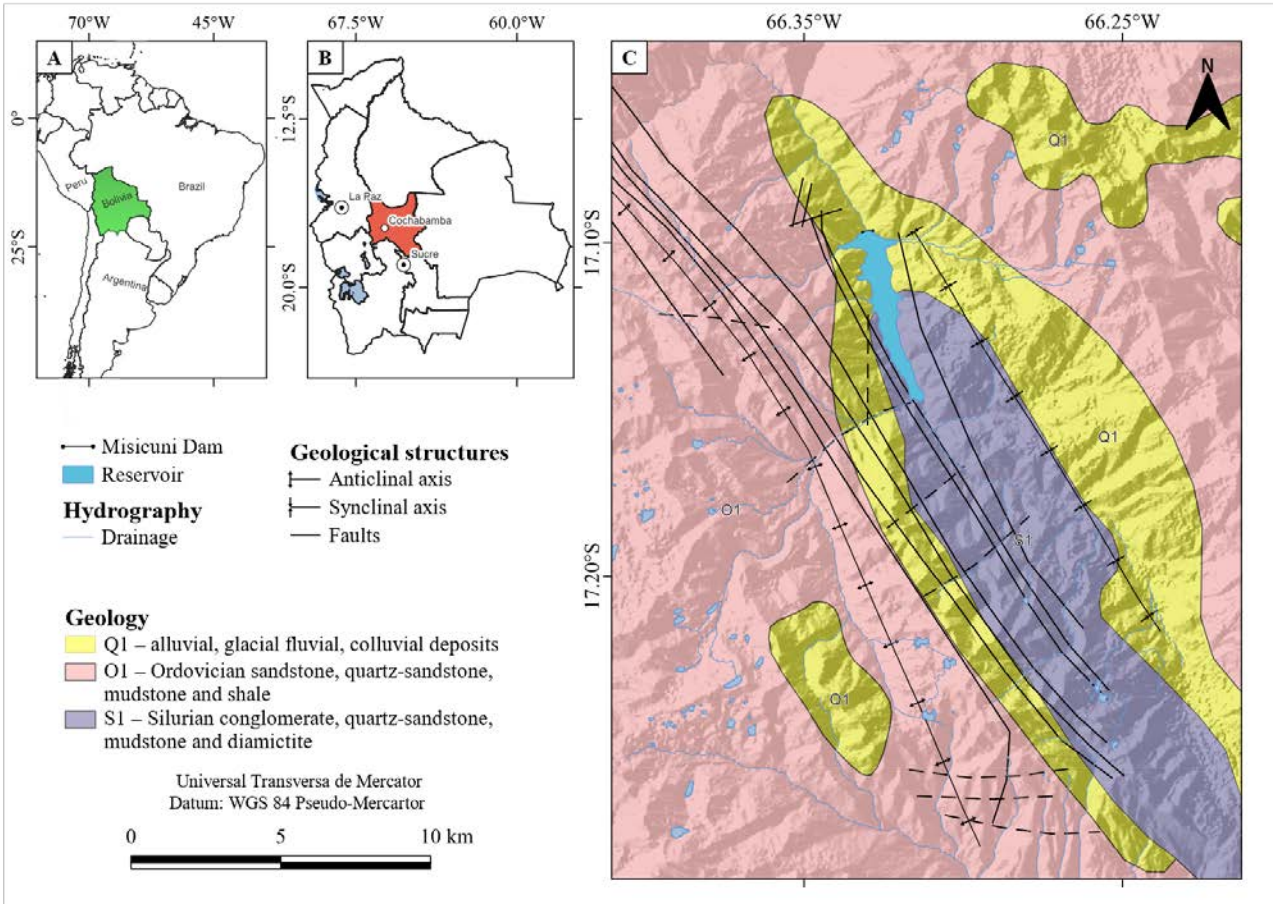

Figure 1 - (A) Location of the study area in South America. (B) Cochabamba's location in Bolivia. (C) Geological map of the Multiple Project. Lithological data extracted from GeoBolivia (geo.gob.bo) and structural geology from Minor et al., 1987.

Figure 2 - General view of the Misicuni Dam and the spillway excavation slope. The red circle shows the location of the excavation slope.

formations are made up of Ordovician rocks (Anzaldo and San Benito Formations), while the lower ones are made up of Silurian rocks (Uncía and Cancañiri Formations). The Ordovician rocks are from marine origin and composed mainly of siltstones, sandstones, shales and mudstones, in a package over 5000 m long. The Silurian sedimentary packages are of glacial-marine origin.

Geology near the spillway

The spillway of the Misicuni dam is located on the hydraulic left bank and excavations over 180 m high were necessary for this implementation. This paper evaluates the stability of the excavation slope between axes 2 and 5 along the spillway with a height of more than 30 m (Figure 3). To establish the geological cross-section for the excavation project, three boreholes were drilled along the highest section. Figure 4 shows the result of the SR-401 drill core, exemplifying the quality of the rock mass finding.

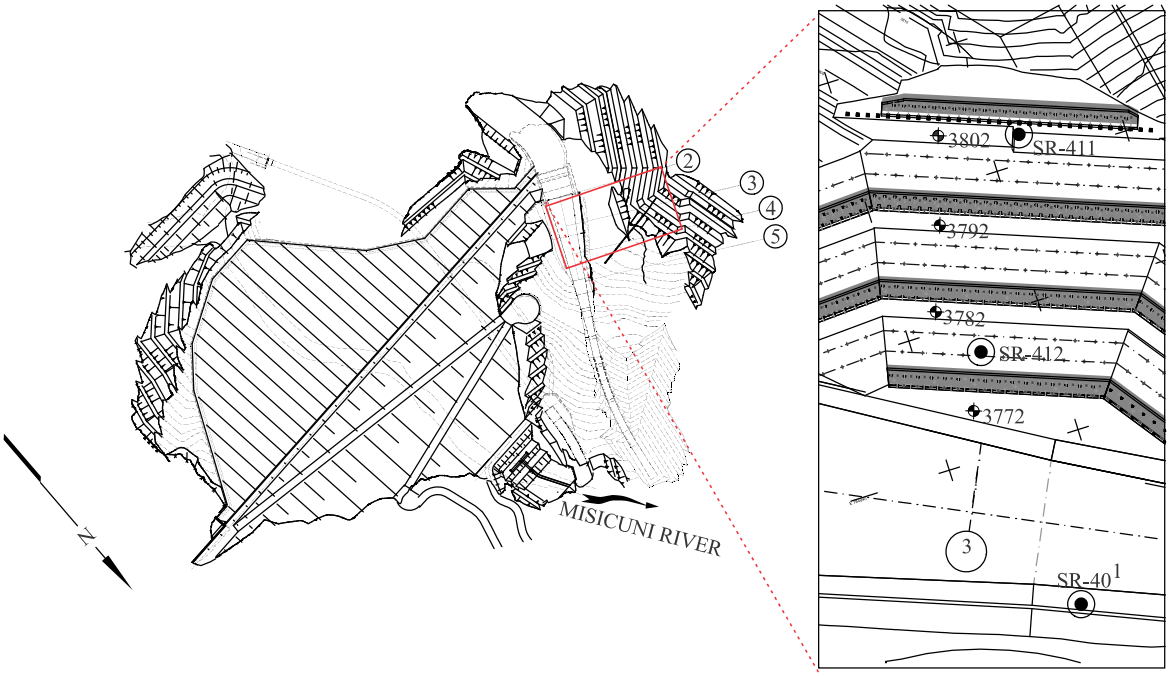

Figure 3 - Plan of the slope and Misicuni Dam, between axes 2 and 5. General arrangement of the excavations and project to stabilize the slope of the Misicuni dam spillway, including location of the boreholes.

Figure 4 - Drill core SR-401 showing the rock mass quality.

The results of the boreholes, as well as field observations made during excavations, made it possible to characterize the rock mass along the section in axis 3. Geotechnical compartmentalization was carried out in terms of the quality of the rock masses and its discontinuities.

The stratigraphy of the excavation slope of the Misicuni Dam spillway is composed of an M-II type rock mass in the lower portion, overlain by an M-III rock mass which is covered by residual soils (Figure 5).

The M-II type rock mass comprises a medium-relieved mass with slightly open, oxidized or semi-decomposed joints and the M-III type is composed of a relieved mass with open joints, decomposed zones and joints with thick silt and clay filling.

Temporary excavations perpendicular to the axis of the embankment in the region of the ogive made it possible to observe the main discontinuities that condition the slope's rupture kinematics, as well as to geotechnically compartmentalize the rock mass. These discontinuities comprise layers of decomposed material or joints with thick clay filling, with extremely altered materials resulting in planes of low resistance.

The images in figure 6 show the details of the fracture planes and filling materials. No friction grooves were observed, assuming that there was no displacement along the planes.

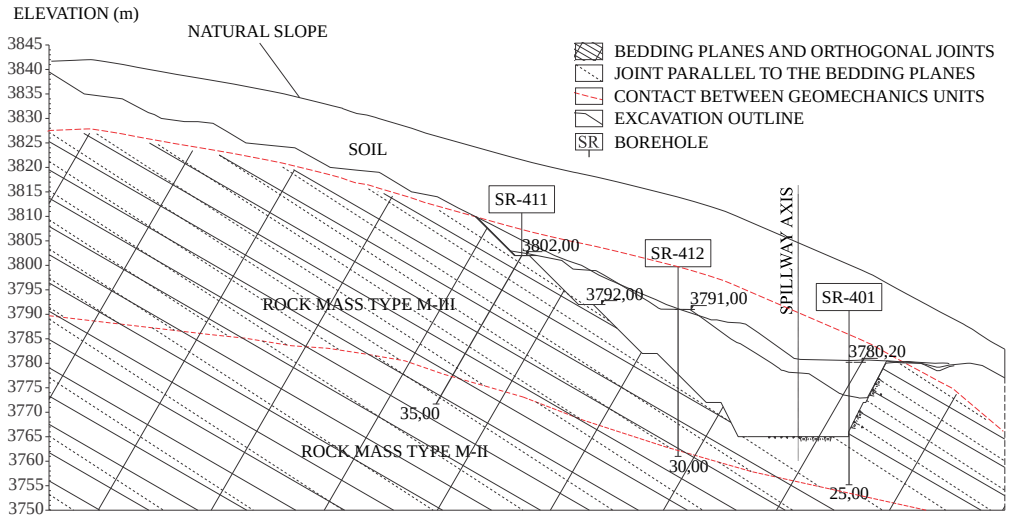

Figure 5 - Geological cross-section on axis 3 with the compartmentalization of the rock masses, excavation of the spillway and boreholes executed.

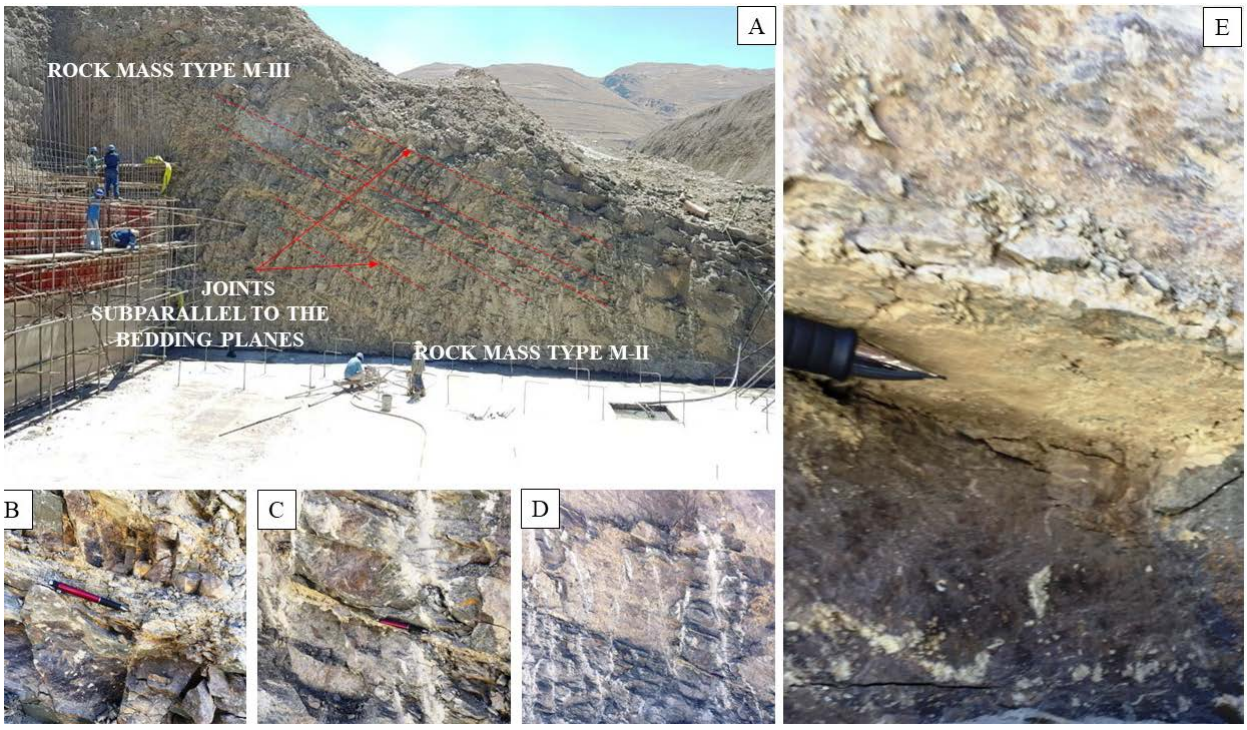

Figure 6 - A) View of the temporary slope perpendicular to the spillway axis during the excavation phase and the division of the masses. B, C, D and E) Detail of the discontinuities showing joints subparallel to the bedding planes and discontinuities with clay filling.

The main discontinuities affecting the slopes of the rock mass between axes 2 and 5 of the spillway are related to the stratification of the sedimentary layers, as well as joints of tectonic origin, joints and faults parallel to the bedding plane. The attitudes of the discontinuities measured in the field are shown in table 1.

The structural measurements were input into the DIPS 6.0 software, where 4 families of discontinuities were observed according to the frequency stereogram, represented by stratification (S_0) and joints (F1, F2, F3). The average attitude (Dip/Dip Direction) of the discontinuities resulted as follows:

- Bedding Plane S_0: 57°/147°
- Joint Unfavorable F1: 36°/106°
- Join F2: 78°/268°
- Join F3: 78°/040°

The structural geology and past landslides during excavations on the left bank showed that the system of discontinuities dipping into the spillway excavation (F1) is unfavorable for stability. Based on the data from the discontinuity attitude measurements, a kinematic analysis was carried out for planar rupture, as shown in figure 7. There is a probability of around 10% for the occurrence of planar rupture along the discontinuities with a dip of between 30 and 35 degrees and towards the inside of the spillway excavation.

Table 1 - Structural measurements collected in the field.

Dip	Dip Direction	Dip	Dip Direction	Dip	Dip Direction
30	120	25	090	60	330
70	270	80	020	80	060
75	330	80	090	75	240
30	100	85	300	60	140
45	120	50	090	70	030
34	120	55	180	60	140
30	120	20	285	75	040
60	150	48	155	80	310
80	270	80	50	83	265
40	240	20	300	47	110
50	290	57	150	85	040
70	160	50	100	30	090
85	150				

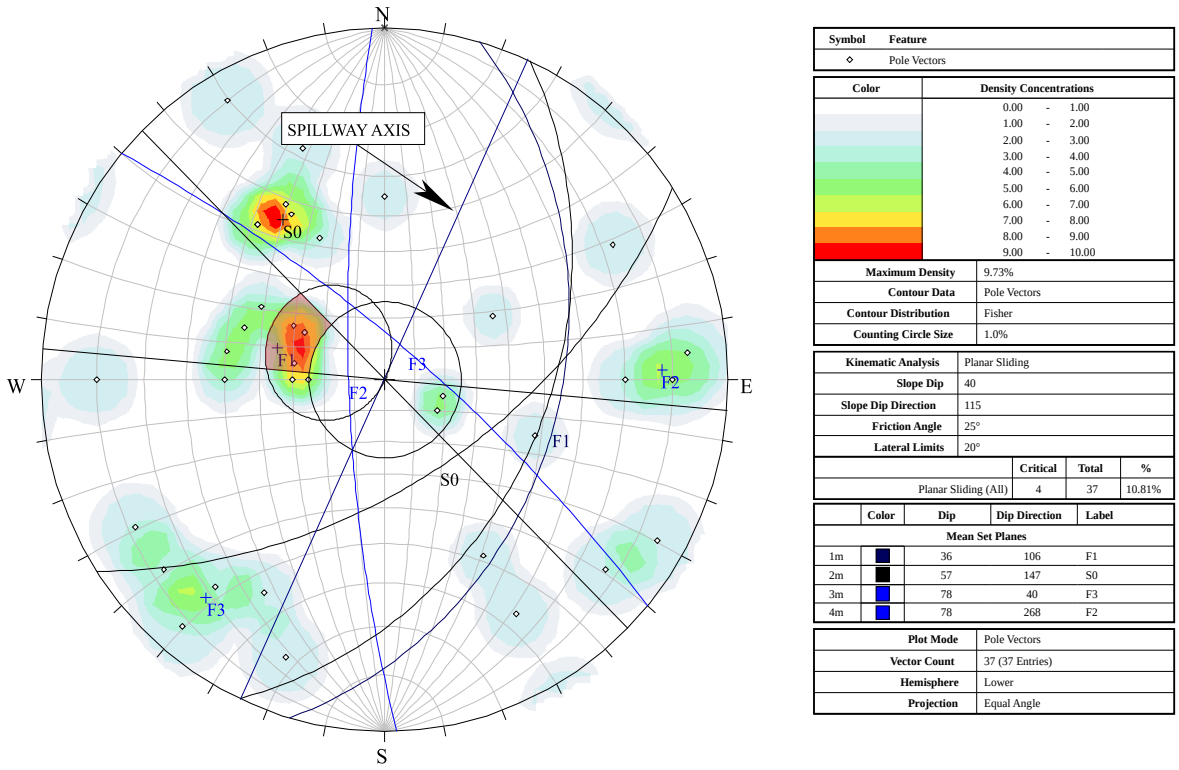

Figure 7 - Frequency diagram of discontinuities and kinematic analysis for planar rupture - Axis 2 to 5.

The resistance parameters along the planes of these fractures were initially estimated based on the limit equilibrium theory, considering that the rock mass was in equilibrium until the first signs of mobilization of the landslide occurred.

For this condition, the resistance parameters adopted for the discontinuity planes were cohesion c = 0 kPa and friction angle 30°, which corresponds to the lowest inclination of the dip of the discontinuity planes.

The discontinuities, combined with the poor geomechanical quality of the M-III rock mass, favored the landslides observed at the spillway site, with planar or mixed ruptures, although these were always conditioned by the surface planes of the discontinuity system.

The design solution adopted for the containment of this slope consists of the construction of a curtain wall intercepting possible rupture planes with tieback.

OBSERVATIONS DURING EXCAVATION AND ANALYSIS OF MONITORING DATA

Instrumentation and excavation

The excavations and installation of the tieback took place throughout the year of 2018 and early 2019 (Figure 8). To monitor the deformations that occurred during this period, two inclinometers were installed aligned on axis 3, one on the bench at elevation 3802 and the other at 3782 m (Figure 9).

The first inclinometer (el. 3802 m), called INCV-01-A, is 37 m long and took its first reading on 26/07/2018, while the second, INCV-04 (el. 3782), is 21 m long and was installed on 28/11/2018. INCV-04 was damaged after the installation of some DHPs.

It was recovered in April 2019 and renamed INCV-04-A, but with a new depth of 19 m, and the deformation readings started over from the origin.

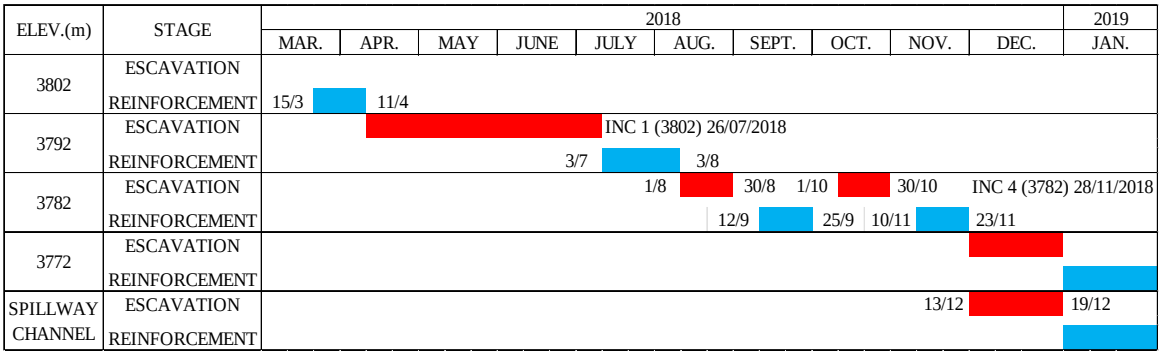

Figure 8 - Excavation control and reinforcement over time.

Inclinometer INCVA-01. INCVA-01 did not have one of its axes aligned with the interior of the excavation, showing high deformations in both the "A" and "B" axes. The graph of the accumulated displacements of INCVA-01 is shown in figure 10 with readings up to September 3, 2020. Two main displacement surfaces were observed, one at a depth of 20.50 m (El. 3781.50) with larger displacements and another at 27.50 m (El. 3774.50) with a smaller magnitude.

During the building period, the accumulated displacements of the resultant vector for the depth of 20.5 m amounted to just over 16 mm and are plotted on a graph of accumulated displacement × time, shown in figure 11. The accumulated displacements of the resultant vector show a constant evolution over time with variations in localized periods, as well as accelerations that show significant increases in the excavation periods and decelerations in periods when excavations were standstill and installation of reinforcements took place.

The readings obtained in the first stage of excavation of 3782 m indicated accumulated deformations of 4.3 mm, which stabilized at 6.5 mm when reinforcements were installed. The excavation of 3772 berm and the canal, show that deformations progressed to 8.8 mm and during anchor load the displacements almost doubled, reaching 16.1 mm. After this stage, with the work completed, the slope of the deformation line reduces drastically, indicating that there were no accelerations after the work was completed. However, over the course of 2019 the accumulated deformations reached 32.7 mm, stabilizing over the course of 2020, reaching 34.9 mm. Behavior like this after the building period has already been observed by Song et al. (2011), and can be explained by rock mass creep, different from rock creep, and it is closely related to slope structure and geological conditions.

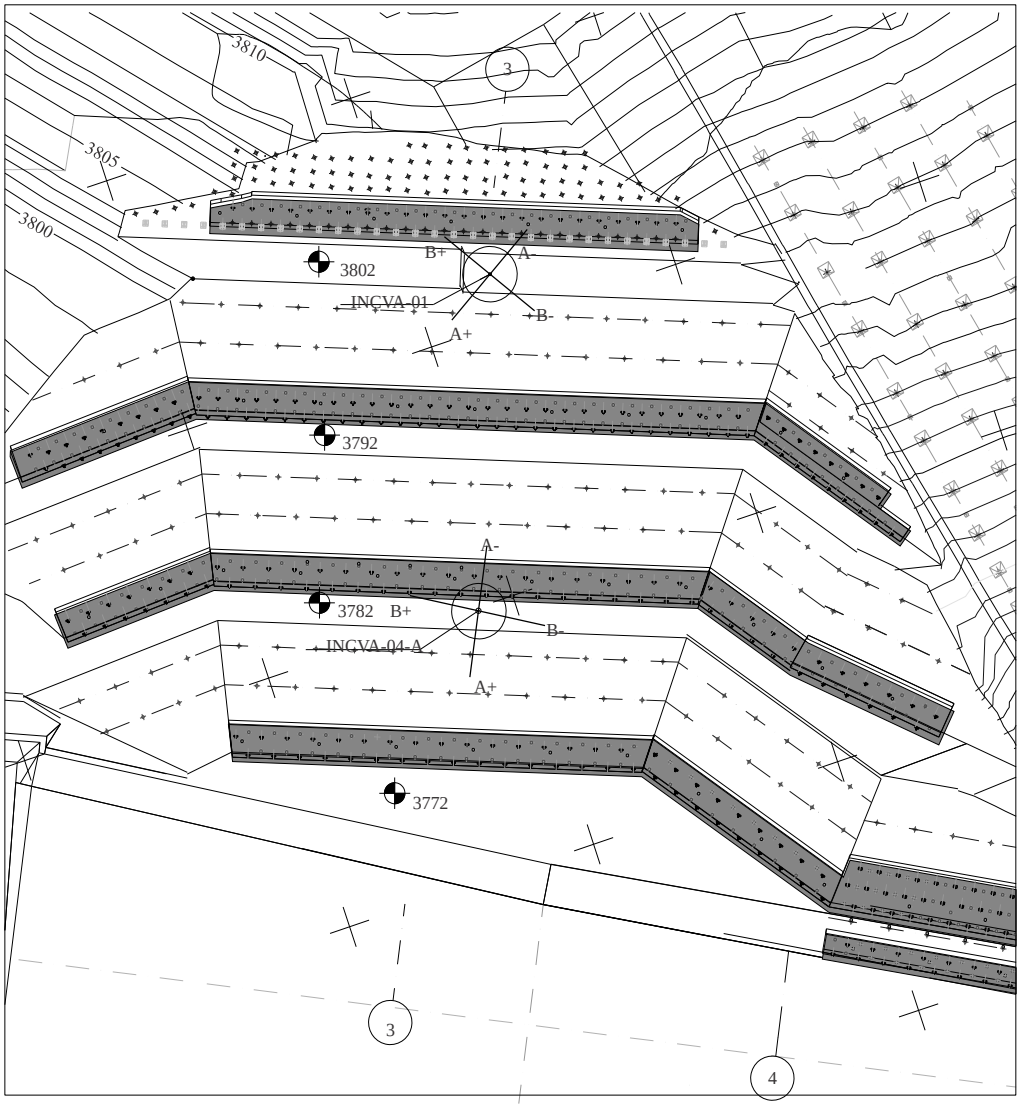

Figura 9 - Plan of the inclinometers location with their reading axes.

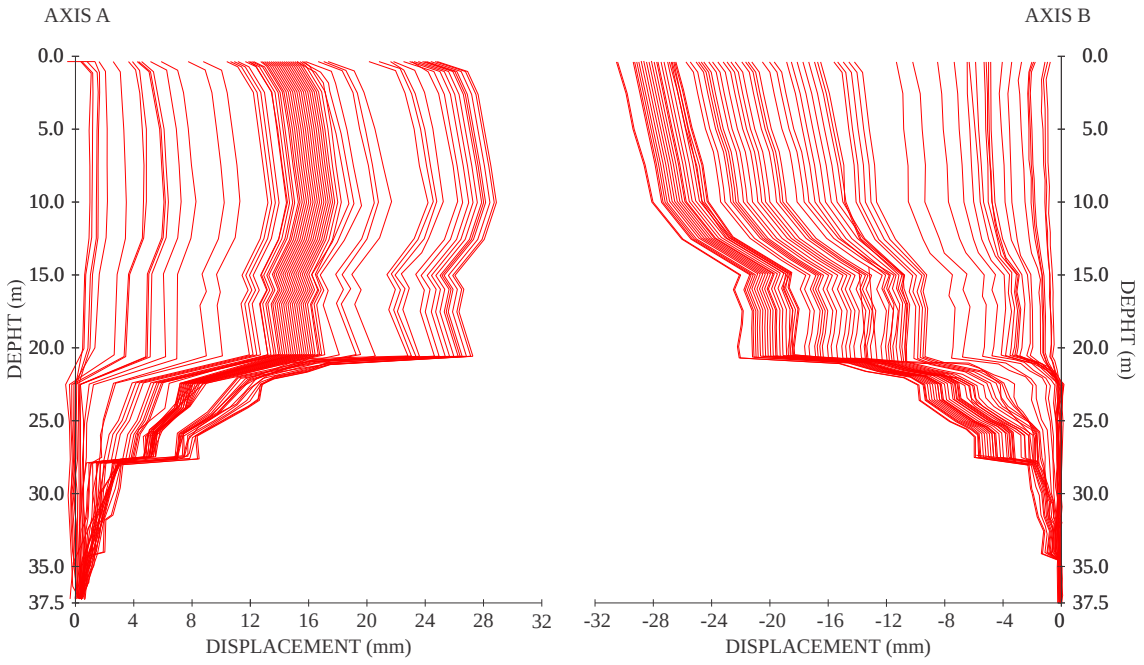

Figura 10 - Cumulative displacements– INCVA-01.

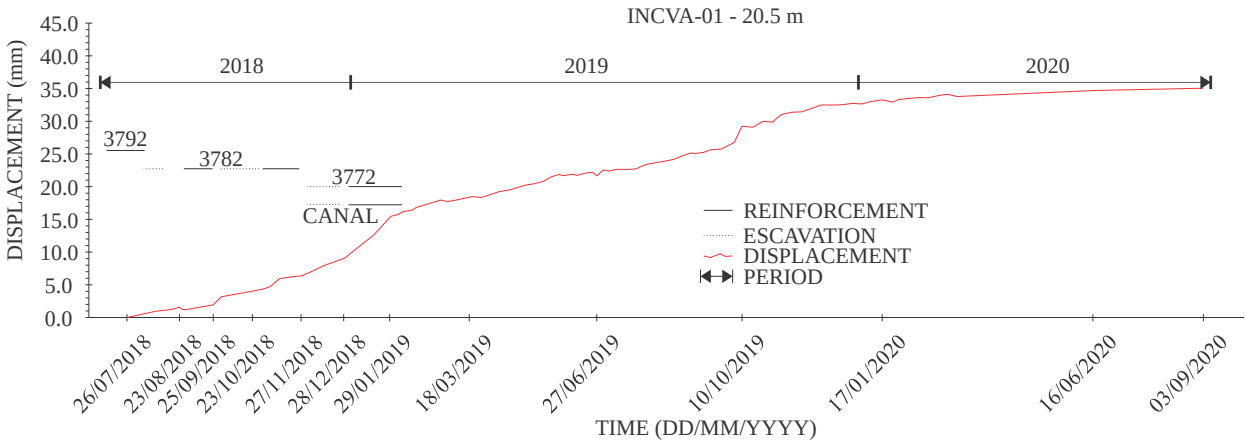

Figure 11 - Cumulative displacement × time INCVA-01 at depth 20.50 m for the building period and residual deformations in 2019 and 2020.

Inclinometer INCVA-04 and INCVA-04-A. There is reading data for INCVA-04 between November 2018 and February 2019.

The accumulated displacement graph of INCVA-04 is shown in figure 12, indicating two deformation planes, the main one at a depth of 12.5 m (El. 3769.50) and another with smaller displacements at a depth of 18 m (El. 3764).

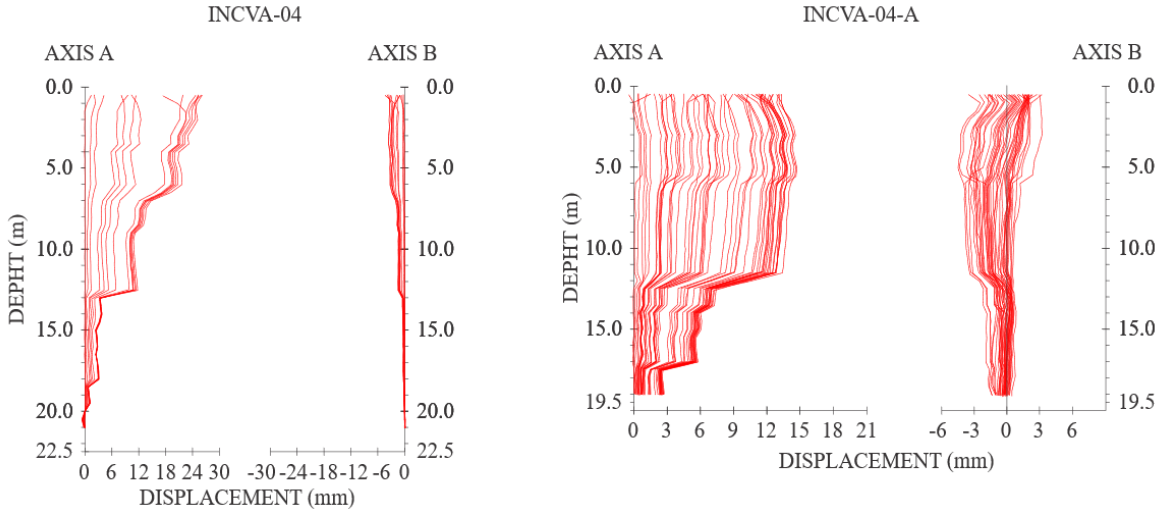

Figure 12 - Cumulative displacement INCVA-04 and INCVA-04-A.

This inclinometer was properly positioned, with the "A" axis aligned towards the inside of the excavation, showing the main deformations only on this axis. The accumulated displacements of the resultant vector for the 12.5 m depth amounted to around 12 mm and were plotted on an accumulated displacement *versus* time graph. The deformations obtained coincide with those observed in INCVA-01, with significant accelerations during excavations and decelerations during periods when excavations were standstill and installation of reinforcements occurred, as seen in figure 13.

With the excavation and prestressing of berm 3782, excavation continued on el. 3772 and the channel. The deformations reached around 4 mm during excavation, and by the end of prestressing the deformations had reached 10 mm, stabilizing at 12 mm after completion of reinforcements installation.

Deep drainages were installed after the bolting, which damaged the INCVA-04 during installation.

In April 2019, repairs were made to the tube of this instrument, and readings were resumed on April 30, 2019, with a new reference, renaming the instrument INCVA-04-A.

The INCVA-04-A reading period includes the residual deformations that occurred after the work was carried out, with readings between 30/04/2019 and 03/09/2020. For this period, the incremental displacement graph of the INCVA-04A inclinometer (Figure 12) indicates that there are 3 movement surfaces, at depths of 11.5 m, 13.5 m and 17 m, which are at similar depths to those previously observed in INCVA-04. Of these surfaces, the main one is at 11.5 m, one meter higher than previously recorded (12.5 m).

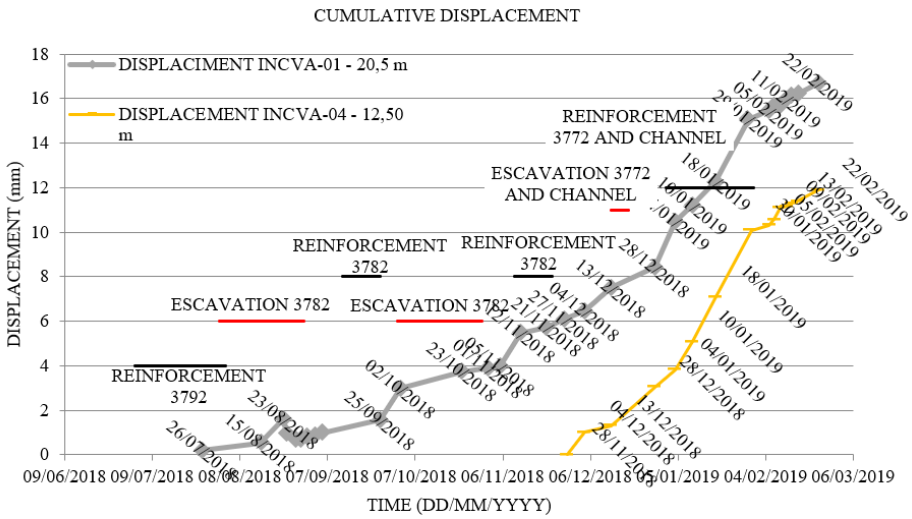

Figure 13 - Cumulative displacement × time INCVA-04 at depth 12.50 m compared to INCVA-01 for the building period.

The cumulative displacement × time graph at a depth of 11.5 m (Figure 14) shows that:

- the period from 09/10/2019 to 26/02/2020, 140 days, shows an accumulated deformation of 13.00 mm - 8.30 mm = 4.7 mm, resulting in an average speed of 0.033 mm/day, already considered residual and tending to stabilize;
- in the period from 26/02/2020 to 16/06/2020, 111 days, the accumulated deformation obtained is 13.00 mm - 12.90 mm = 0.10 mm, resulting in an average speed of 0.0009 mm/day;
- In the period from 16/06/2020 to 03/09/2020, 79 days, the accumulated deformation obtained is 13.54 mm - 12.90 mm = 0.64 mm, resulting in an average speed of 0.008 mm/day.

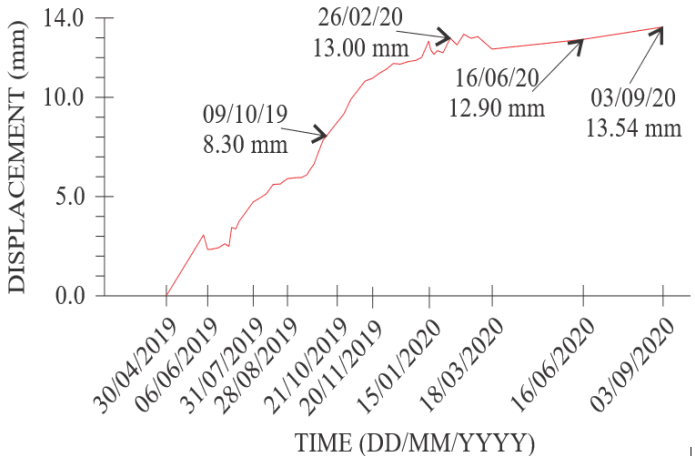

Figure 14 - Cumulative displacement × time – INCVA-04-A at depth 11,5 m.

STRESS-STRAIN ANALYSIS

Numerical analysis

Numerical modeling is widely used to solve various problems related to geotechnical engineering projects.

In this study, the stress × strain analyses were carried out using the Phase2® v8.0 software (rocscience), which allows the displacements during the excavation and bolting phases to be evaluated using the finite element method (FEM) and the slope safety factor to be obtained from the SSR.

The model design for this type of assessment considers various factors, the main ones being: geometry, material parameters, construction sequence and an understanding of geological complexity.

For soft and tectonically affected sedimentary rocks, slope stability is mainly dominated by the variability of the materials and geological structures that condition the sliding surface, which always tends to seek out the materials with the lowest resistance (Ahmed & Soubra, 2012; Fenton & Griffiths, 2008; Zeng et al., 2015; Cheng et al., 2016, 2017, 2018).

The data from the inclinometers made it possible to evaluate the behavior of the deformation and estimate the possible rupture surfaces. Instrumentation similar to this provides

extensive knowledge of the geological characteristics that condition deformations and failure modes and has been used to monitor excavations on extremely high slopes related to hydroelectric power generation sites (e.g., Chen et al., 2016; Chen et al., 2017; Xu et al., 2017).

Numerical analysis was used to estimate the resistance parameters based on the deformations observed during the excavation and support application stages. Figure 15 shows the geological model used and the phases of excavation and application of the ties during the building period.

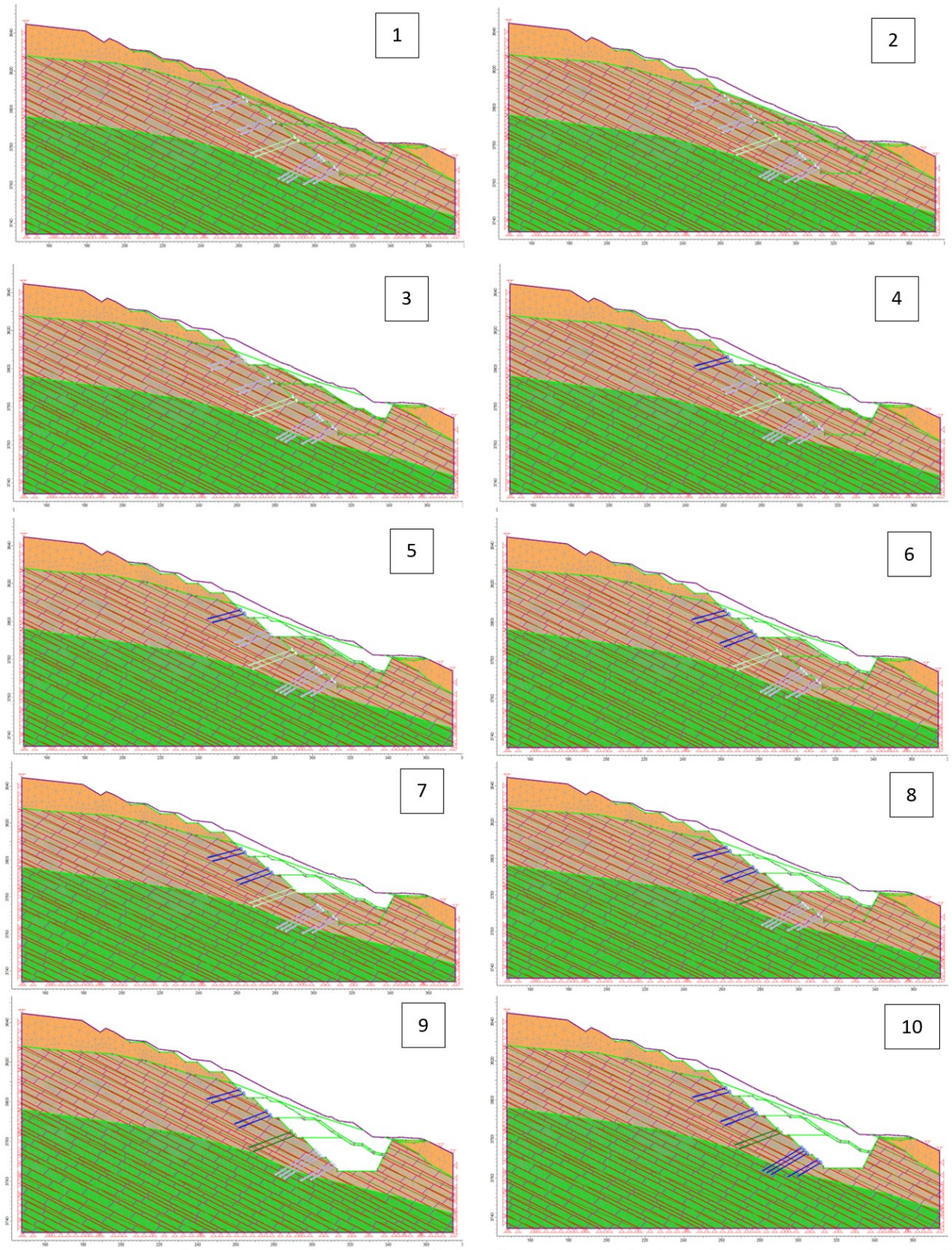

Figure 15 - Construction sequence of the slope carried out in 10 stages with alternating excavation and application of the designed support.

The external geometry of the model was based on the topographic surveys carried out prior to the first excavations, and the other steps according to the subsequent topographic surveys, design drawings and support installations carried out.

The stratigraphy of the proposed geological model was drawn up on the basis of surface mapping, boreholes along the section and mapping of the excavation front, which exposed the main structures that condition the slopes rupture kinematics. In view of this geological context, discontinuities such as bedding, orthogonal joints and faults were inserted into the model according to the mappings carried out.

The modeling included 10 construction stages, the first containing the previous conformation of the relief prior to the excavation of the bench at elevation 3802, and the last with the conclusion of the excavation and installation of the ties near the spillway chute. Since the inclinometer was installed after the excavation of the 3802 bench had been completed, the deformations were set to zero from this stage onwards (3rd stage) in order to make the model compatible with the deformations observed in INCVA-01.

The strength parameters were assessed and obtained mainly on the basis of the final deformations observed in the INCVA-01. This instrument is the most representative of the deformations observed and returned values of around 35 mm at the end of construction.

The deformations that occur during the excavation and anchoring process are generally more complex to model, as the readings taken in the field are daily based and do not necessarily represent the same deformations that were observed in the model. This is due to the temporal conditions of the readings, and it is preferable, for greater accuracy in these types of analyses, that the readings are automated and in real time.

ESTIMATION OF PARAMETERS AND DEFORMATIONS

The geomechanical properties of the rock masses were initially estimated based on the literature and the authors' experience with lithotypes and investigations carried out in similar geological contexts, as well as uniaxial compression tests carried out at the dam site.

In addition to the rock mass, it was necessary to estimate resistance parameters for the sedimentary bedding, the set of orthogonal joints and the faults parallel to the bedding planes.

As the curtain wall is a known material, the parameters supplied by the manufacturer were used.

Table 2 shows the estimated parameters for the rock mass and discontinuities included in the model.

Table 2 - Parameters of the rock masses and discontinuities.

Parameters	Unit	Material					
		Soil	M-III	M-II	Bedding plane	Orthogonal joint	Parallel faults to bedding planes
Elastic modulus	GPa	0.5	1.28	2	-	-	-
Poisson's ratio	-	0.28	0.28	0.28	-	-	-
Unit weight	kN/m³	21	26	26	-	-	-
Cohesion	MPa	0.02	-	-	0.012 (0.010*)	0.1 (0.05*)	0
Friction angle	º	36	-	-	20 (18*)	39 (34*)	10 (7*)
Normal stiffness of the joint	GPa/m	-	-	-	1.2	1.41	1
Shear stiffness of the joint	GPa/m	-	-	-	0.5	0.47	0.1
GSI	-	-	40	40	-	-	-
UCS	MPa	-	30	68	-	-	-
mi	-	-	13	17	-	-	-
D	-	-	0	0	-	-	-

(*) Residual Values

Parameter estimates for the rock masses were based on the Hoek & Brown (1980) criteria and for the topsoil the Mohr-Coulomb criterion was used. The M-II material is a relieved mass with slightly open, oxidized or semi-decomposed fractures and the M-III is a relieved mass with open fractures, decomposed zones and fractures with thick silt and clay filling.

Parameter estimation is initially based on the GSI (Geological Strength Index; Hoek 1994), which qualitatively assesses mass quality quickly and economically based on the degree of fracturing and alteration of discontinuities.

For the masses evaluated, the estimated GSI

(Geological Strength Index) was 40 for both masses, where only the discontinuities of the sedimentary bedding were considered, being the same for both units.

The difference in the model occurs in the insertion of faults parallel to the bedding (F1), where those present in mass M-III have a smaller spacing between them than in M-II, thus representing mass M-III as a more fractured unit.

The bedding planes and the orthogonal joints were inserted as "cross jointed", with an average spacing of 3 m for the bedding planes and 12 m for the orthogonal joints.

The discontinuity system was applied as parallel deterministic with an inclination of 33º and a spacing of 10 m for the M-II and 5 m for the M-III mass.

The main factor governing the differences between the strength parameters of the rock masses in the model reflects data obtained from the simple compressive strength tests (Table 3), which showed an average of 68 MPa, assumed for M-II, and a minimum of 26 MPa, with 30 MPa being adopted for M-III.

Table 3 - Results of the uniaxial compression tests.

Uniaxial Compressive Strength Tests									
Samples				σ_c	Samples				σ_c
Hole	Depth		Rock	MPa	Hole	Depth		Rock	MPa
S-101	1.50	1.50 - 1.70	Siltstone	54.90	S-106	11.60	11.60 - 11.80	Siltstone	101.00
S-101	6.50	6.50 - 6.70	Siltstone	69.10	S-106	18.20	18.20 - 18.50	Mudstone	48.80
S-101	14.30	14.30 - 14.50	Siltstone	71.10	S-106	45.60	45.60 - 46.00	Mudstone	69.10
S-101	27.30	27.3 - 23.90	Siltstone	54.90	S-106	55.80	55.80 - 56.10	Mudstone	48.80
S-101	30.60	30.60 - 31.00	Siltstone	90.90	S-107	9.50	9.50 - 9.65	Siltstone	63.00
S-101	37.60	37.60 - 37.80	Siltstone	77.20	S-107	20.85	20.85 - 21.00	Mudstone	104.40
S-102	13.10	13.10 - 13.30	Siltstone	42.70	S-107	26.50	26.50 - 26.80	Siltstone	48.80
S-102	14.80	14.80 - 15.00	Siltstone	114.60	S-107	39.30	39.30 - 39.50	Siltstone	77.20
S-102	22.50	22.50 - 22.35	Siltstone	77.20	S-108	3.80	3.80 - 4.00	Siltstone	125.30
S-102	27.60	27.60 - 27.80	Siltstone	103.30	S-108	15.60	15.60 - 15.80	Siltstone	52.80
S-102	33.50	33.50 - 33.80	Siltstone	77.20	S-108	31.50	31.50 - 31.70	Siltstone	77.20
S-103	32.30	32.30 - 32.50	Siltstone	26.40	S-108	35.30	35.30 - 35.50	Siltstone	65.00
S-103	35.20	35.20 - 35.50	Siltstone	40.60	S-108	40.50	40.50 - 40.80	Siltstone	75.20
S-103	39.20	39.20 - 39.50	Siltstone	35.60	S-108	47.25	47.25 - 47.40	Siltstone	41.00
S-104	6.30	6.30 - 6.50	Siltstone	60.90	S-108	50.20	50.20 - 50.40	Siltstone	38.60
S-104	10.20	10.20 - 10.40	Siltstone	42.70	S-108	59.60	59.60 - 59.80	Siltstone	63.00
S-105	5.00	5.00 - 5.50	Siltstone	56.90	S-108	62.10	62.10 - 62.40	Siltstone	110.00
S-105	9.50	9.50 - 10.00	Siltstone	63.00	S-108	67.60	67.60 - 67.80	Siltstone	67.00
S-105	16.60	16.60 - 16.80	Siltstone	48.80	S-108	70.80	70.80 - 71.00	Siltstone	111.70
S-105	43.00	43.00 - 43.15	Siltstone	71.10					
Maximum				125 MPa					
Average σ_c				68 MPa					
Minimum				26 MPa					

For the FEM, the modulus of deformability is the main parameter that determines deformations, especially in rock masses that are not very fractured. Even though this is a fractured mass, the modulus of deformability was estimated using RocLab® (Rocscience), taking as input the uniaxial compressive strength, the GSI, the excavation disturbance factor and an estimate of the modulus of deformation of the intact rock. The specific weight of the materials was estimated based on the lithology, and this is a parameter that generally has a strong influence on deformations. However, due to the local geological context, it is the discontinuities present in the masses that mainly condition deformations and possible rupture.

One of the greatest difficulties in developing models with joints is representing the orientations, spacing along the section and obtaining parameters for these materials. In particular, the shear and normal stiffness module, introduced by Goodman (1968), which are difficult to test in laboratory and are of major importance for finite element analysis.

Data presented by Day et al. (2017), Sattler & Paraskevopoulou (2019), Asem & Gardoni (2019), Clayton et al. (2020) and Zheng et al. (2023), indicate that the order of magnitude of

the shear or normal stiffness can range from 0.1 GPa/m to 100 GPa/m. Bearing in mind that high values for the modulus of stiffness restrict deformations and low values show excessive deformations, it was decided to set these parameters in ranges reported in the literature for similar discontinuities.

In this way, the parametric analysis of the faults that condition the deformations in the slope was carried out by varying the angle of friction, because, as this is a set of faults, the premise is that cohesion is zero. Based on the characteristics observed in the excavations, the fill is clay, and possibly has a low friction angle, making it necessary to reduce the peak friction to 10º and the residual friction to 7º in order to obtain the deformations observed in the inclinometers (Figure 16).

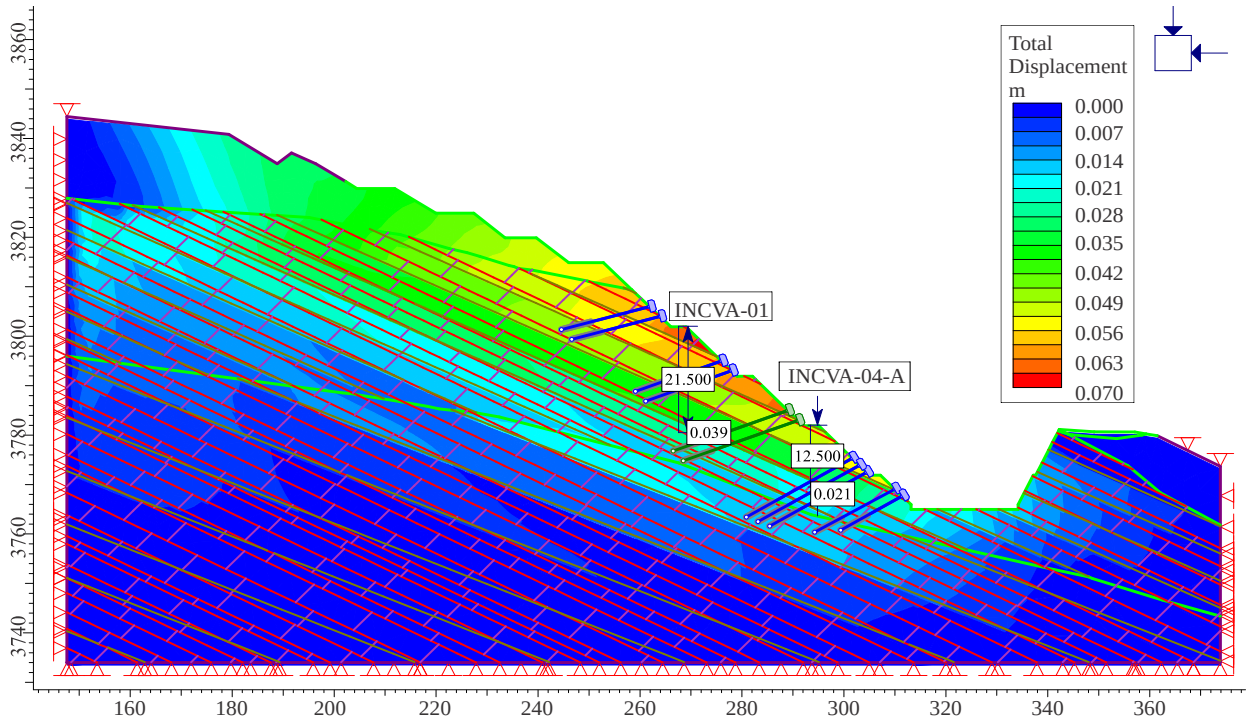

Figure 16 - Final model with the deformations observed in INCVA-01 (39 mm) and INCVA-04A (21 mm).

For the joints orthogonal to the bedding, relatively high spacing was adopted, which is not what was observed in the field. This was necessary because small spacings generate blocks with large deformations in the model, indicating the possibility of localized rupture. To simulate global rupture based on the deformations obtained from the inclinometers, the adopted parameters for the orthogonal joints were less conservative so that the deformations were concentrated on the displacement surfaces observed in the INCVA-01 and INCVA-04 and 04-A inclinometers.

The deformation obtained in the model was 39 mm, which is very similar to the deformation observed in INCVA-01 after the relaxation period of the mass.

The final reading obtained in INCVA-04-A was around 12 mm, while the model showed a value of 21 mm. This difference is probably related to the installation period of INCVA-04-A, which could only take its initial readings after the excavation of the 3782 m bench had been completed.

Thus, based on the rupture model used for the mass found in the excavation of the Misicuni dam spillway and the deformations measured and calculated, it can be concluded that the estimated parameters are adequate and show good agreement, as well as being supported by data presented in relevant bibliographies on the subject.

CONCLUSIONS

This paper presents the deformation modeling of a historical case of rock slope stabilization in the Andean region. The excavations were carried out in a rock mass of low geomechanical quality and high geological complexity. The final deformations were quantified using readings from inclinometers installed on the slope and the geomechanical model designed was based on bore-

holes executed in the analysis section and mapping performed during the excavation period.

The rocks found at the dam site comprise siltstones, sandstones and mudstones with sedimentary bedding inclined at around 30 to 35º and a set of joint parallel to the bedding. Structural measurements and minor landslides during excavation of the left bank showed discontinuities with an unfavorable dip to stability, indicating a probability of approximately 11% of planar rupture along the discontinuities towards the interior of the excavation.

Reinforcing anchors were used to stabilize the slope. They were installed immediately after the excavation of the bench and were of sufficient length to intercept the surface of rupture and prevent major displacements. The parameters were estimated based on geomechanical classifications and uniaxial compression tests at the dam site and re-evaluated using the deformations obtained during the building phase.

The strength of the intact rock is an important factor in obtaining the strength parameters of the rock mass. The uniaxial compression tests on samples collected at the dam site indicated maximum values of 125 MPa and minimum values of 26 MPa, with an average of 68 MPa in the siltstone and mudstone samples tested.

The inclinometers installed indicated accumulated deformation at the end of the construction period of 34.9 mm at elevation 3781.50 m and 13.54 mm at elevation 3770.5 m. These deformations, as well as the structural measurements, were used to estimate the material parameters and the displacement surface.

The input parameters in FEM have a strong influence on deformations, however, it was observed during the analyses that the design of the geological model for deformation and slope stability analyses is extremely important and that a few variations in the orientations of the discontinuities have a more significant impact on deformations than the variability of the parameters. In this way, the geological understanding and mapping of the materials of the masses contributes for a more accurate assessment of the conditions of the rupture surfaces and predicted deformations.

The measurements obtained from the instruments associated with the geological model made it possible to estimate the resistance parameters of the materials found in the excavation of the Misicuni dam spillway. The assumed parameters were consistent with the data reported in the consulted bibliography and the calculated rupture surface corresponded to the deformations observed in the inclinometers. Data provided in this case study and presented in this paper may be useful for engineering projects in similar geological contexts.

REFERENCES

AHMED, A. & SOUBRA, A. Probabilistic analysis of strip footings resting on a spatially random soil using subset simulation approach. **Georisk Assess Manag Risk Syst GeoHazards**, v. 6, n. 3, p. 188–201, 2012.

ASEM, P. & GARDONI, P. Bayesian estimation of the normal and shear stiffness for rock sockets in weak sedimentary rocks. **International Journal of Rock Mechanics and Mining Sciences**, v. 124, p. 104129, 2019.

CHEN, Z.; WANG, Z.; XI, H.; YANG, Z.; ZOU, L.; ZHOU, Z.; ZHOU, C. Recent advances in high slope reinforcement in China: Case studies. **Journal of Rock Mechanics and Geotechnical Engineering**, v. 8, n. 6, p. 775-788, 2016

CHEN, T.; DENG, J.; SITAR, N.; ZHENG, J.; LIU, T.; LIU, A.; ZHENG, L. Stability investigation and stabilization of a heavily fractured and loosened rock slope during construction of a strategic hydropower station in China. **Engineering Geology**, v. 221, p. 70-81, 2017.

CHENG, H.; CHEN, J.; CHEN, R.; CHEN, G.; ZHONG, Y. Risk assessment of slope failure considering the variability in soil properties. **Computers and Geotechnics**, v. 103, p. 61-72, 2018.

CLAYTON, C.; JACKSON, A.; PRICE, J.; BIDWELL, A.; ELMO, D. Case study: Analysis of a highwall toppling failure and development of a successful mine re-entry plan using RS2, RocFall and Dan-W at a coal mine in Canada. In: INTERNATIONAL SYMPOSIUM ON SLOPE STABILITY IN OPEN PIT MINING AND CIVIL ENGINEERING - SLOPE STABILITY, 2020, Crawley, Australia. **Proceedings...** Crawley: Australian Centre for Geomechanics. 2020, p. 383-398.

DAY, J.J.; DIEDERICHS, M.S.; HUTCHINSON, D.J. **Investigating normal and shear stiffness properties of fractures and healed sedimentary nodular structure in the Cobourg limestone**. 2017.

FENTON, G. A. & GRIFFITHS, D.V. **Risk assessment in geotechnical engineering**. New York: John Wiley & Sons., 2008.

GOODMAN, R.E.; TAYLOR, R.L.; BREKKE, T.L. A model for the mechanics of jointed rock. **Journal of the Soil Mechanics and Foundations Division,** v. 94, n. 3, p. 637-659, 1968.

HOEK, E. Strength of rock and rock masses. **ISRM News Journal**, v. 2, n. 2, p. 4-16, 1994.

HOEK, E. & BROWN, E.T. Empirical strength criterion for rock masses. **Journal of the geotechnical engineering division**, v. 106, n. 9, p. 1013-1035, 1980.

JANSEN, R.B. **Dams and public safety**. US Department of the Interior, Bureau of Reclamation. 1983.

LEAL, J.R.; FERREIRA, J.A.; SCHMIDT, F.S.; GERMANO, E.O. Innovative Design Features of the Misicuni CFRD in Bolivia. **The International Journal on Hydropower & Dams**, v. 19, Issue 1, 2012.

MINOR, H.E., CLARKE, I.D.; RIEMER, W. Design of the Misicuni scheme in Bolivia. **Water Power and Dam Construc**tion, v. 39, p. 13-18, 1987.

PEREIRA, G.M. **Acidentes e rupturas de barragens de armazenamento de água**. São Paulo: ABGE. 2020.

ROCSCIENCE. **Roclab Program v 1.0**. Toronto, Canada. 2004.

ROCSCIENCE. **Dips 6.0, Analyze Orientation-Based Geolo-**

gical Data. RocScience's User's Guide, Toronto, Canada.

ROCSCIENCE. **Phase^2. 2D finite element program for calculating stresses and estimating support around the underground excavations**. Geomechanics software and research, Rocscience, Toronto, Canada.

ROJAS VERA, E.; GIAMPAOLI, P.; GOBBO, E.; ROCHA, E.; OLIVIERI, G.; FIGUEROA, D. Structure and tectonic evolution of the Interandean and Subandean Zones of the central Andean fold-thrust belt of Bolivia. In: **Andean tectonics**. Elsevier, p. 399-427, 2019.

SATTLER, T. & PARASKEVOPOULOU, T.S.C. Implications on characterizing the extremely weak sherwood sandstone: case of slope stability analysis using SRF at two oak quarry in the UK. **Geotechnical and Geological Engineering**, v. 37, p. 1897-1918, 2019.

SONG, S.; CAI, D.; FENG, X.; CHEN, X.; WANG, D. Safety monitoring and stability analysis of left abutment slope of Jinping I hydropower station. **Journal of Rock Mechanics and Geotechnical Engineering**, v. 3, n. 2, p. 117-130, 2011.

XU, N.; WU, J.; DAI, F.; FAN, Y.; LI, T.; LI, B. Comprehensive evaluation of the stability of the left-bank slope at the Baihetan hydropower station in southwest China. **Bulletin of Engineering Geology and the Environment**, v. 77, n. 4, p. 1567-1588, 2017.

ZENG, P.; JIMENEZ, R.; JURADO-PIÑA, R. System reliability analysis of layered soil slopes using fully specified slip surfaces and genetic algorithms. **Engineering Geology**, v. 193, p. 106-117. 2015.

ZHENG, Y.; CHEN, C.; MENG, F.; FU, X.; YUAN, W. Smart and fast reinforcement design for anti-dip bedding rock slopes. **Journal of Rock Mechanics and Geotechnical Engineering**, v. 15, n. 11, p. 2943-2953, 2023.

Submetido em 29 de novembro de 2024
Aceito para publicação em 10 de fevereiro de 2025